Cone Beam and Micro-Computed Tomography Validation of Manual Array Insertion for Minimally Invasive Cochlear Implantation

Wilhelm Wimmer[a]   Brett Bell[a]   Markus E. Huth[b]   Christian Weisstanner[c]
Nicolas Gerber[a]   Martin Kompis[b]   Stefan Weber[a]   Marco Caversaccio[a, b]

[a]ARTORG Center for Biomedical Engineering Research, University of Bern, and [b]Department of ENT, Head and Neck Surgery, and [c]Institute of Diagnostic and Interventional Neuroradiology, Inselspital, University of Bern, Bern, Switzerland

Abstract

Delivering cochlear implants through a minimally invasive tunnel (1.8 mm in diameter) from the mastoid surface to the inner ear is referred to as direct cochlear access (DCA). Based on cone beam as well as micro-computed tomography imaging, this in vitro study evaluates the feasibility and efficacy of manual cochlear electrode array insertions via DCA. Free-fitting electrode arrays were inserted in 8 temporal bone specimens with previously drilled DCA tunnels. The insertion depth angle, procedural time, tunnel alignment as well as the inserted scala and intracochlear trauma were assessed. Seven of the 8 insertions were full insertions, with insertion depth angles higher than 520°. Three cases of atraumatic scala tympani insertion, 3 cases of probable basilar membrane rupture and 1 case of dislocation into the scala vestibuli were observed (1 specimen was damaged during extraction). Manual electrode array insertion following a DCA procedure seems to be feasible and safe and is a further step toward clinical application of image-guided otological microsurgery.

© 2013 S. Karger AG, Basel

Introduction

Since the inception of cochlear implants (CI), the facial recess approach has become the standard surgical technique to access the tympanic cavity and the cochlea. Currently, safe implant insertion through the facial recess generally requires a substantial mastoidectomy. Though the facial recess approach has remained largely unaltered, steps have been made toward reduced invasiveness (e.g. through the introduction of small incisions or microendoscopic procedures [Hiraumi et al., 2013]). Furthermore, alternative surgical approaches utilizing the external auditory canal (EAC) to pass the CI electrode array into the tympanic cavity have been proposed. For example, the suprameatal, transcanal or pericanal approaches have drawbacks such as a steepened insertion angle, leading to a higher risk of electrode array kinking or damage to intracochlear structures [Zeitler and Balkany, 2010]. Further, the risk of inflammation or infection of the EAC skin, and of consecutive electrode array extrusion, is increased.

Conversely, several methods of achieving a minimally invasive posterior tympanotomy or direct cochlear access (DCA) have been proposed. These methods aim to avoid wide mastoidectomies while at the same time targeting the cochlea, for instance at the round window (RW), at an op-

Wilhelm Wimmer
ARTORG Center for Biomedical Engineering Research
University of Bern, Murtenstrasse 50
CH–3010 Bern (Switzerland)
E-Mail wilhelm.wimmer @ artorg.unibe.ch

timal geometric angle relative to the basal turn. In this context, patient-specific stereotactic templates [Balachandran et al., 2010; Labadie et al., 2008] and skull-mounted [Kobler et al., 2012; Kratchman et al., 2011] or more conventional image-guided robotic approaches [Baron et al., 2010; Klenzner et al., 2009] have been presented. Our group recently demonstrated that a DCA tunnel (1.8 mm in diameter) could be drilled with a targeting accuracy of 0.15 ± 0.08 mm using an image-guided robotic system [Bell et al., 2013]. As opposed to electrode array insertion through conventional mastoidectomy under direct visual feedback using standardized insertion tools, insertion through small tunnel holes is more demanding due to restricted access for visual inspection and maneuvering of the electrode array. Thus, specific insertion tools, for both automatic and manual insertion, have been proposed [Hussong et al., 2010; Kratchman et al., 2012]. However, to our knowledge, no clinical data have been published on the effectiveness of such insertion tools.

Therefore, this study investigates the feasibility and efficacy of manually inserting a free-fitting CI electrode array through a minimally invasive DCA tunnel. We hypothesize that the electrode array can be threaded through the DCA tunnel and advanced into the cochlea utilizing common otological surgical instrumentation. The efficacy of the insertion is assessed by postoperative radiological evaluation of the implant position, the insertion depth angle and the alignment of the DCA trajectory, using cone beam computed tomography (CBCT). Further, the extent of intracochlear trauma is evaluated by means of micro-computed tomography (micro-CT) imaging.

Materials and Methods

Surgical Preparation
As specimens, 4 Thiel-fixed human cadaver heads (n = 8 temporal bones) were used in this study [Thiel, 1992]. Preceding the actual insertion experiment, 1.8-mm-diameter DCA tunnels were drilled in each temporal bone of the specimens, using an image-guided robotic approach [Bell et al., 2013]. In short, titanium screws were placed in each temporal bone of the specimens to establish fiducial landmarks. Then, the specimens underwent CBCT imaging to permit trajectory planning [Gerber et al., 2013a] and high-accuracy patient-to-image registration [Gerber et al., 2013b]. Ultimately, the robotic system drilled a DCA tunnel from the surface of the mastoid bone through the facial recess to the center of the RW, as defined in the preoperative plan (fig. 1).

The insertion study was carried out by first creating a conventional tympanomeatal flap through a retroauricular incision in order to provide access to and visibility of the cochlear promontory and the RW niche. Under microscopic view, the correct alignment of the DCA target relative to the RW was confirmed using an oto-
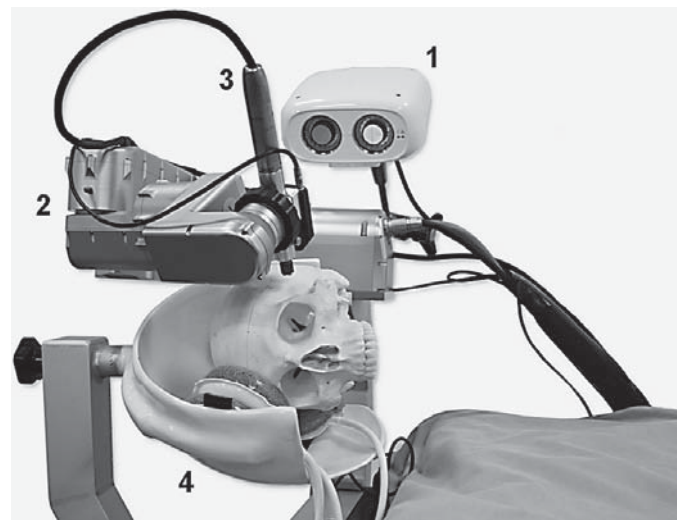

Fig. 1. Imaged-guided robotic system for DCA consisting of a high-accuracy optical tracking camera (1), robotic arm (2), surgical drill (3) and noninvasive head clamp (4).

logical microneedle. The RW membrane was visualized by removing the bony overhang of the subiculum with a 1-mm otological Skeeter drill (Medtronic Xomed, USA). Bone dust was removed from the DCA tunnel and the promontory with saline irrigation and aspiration (1-mm suction tube). Additionally, a 1-mm-diameter sialendoscope (Karl Storz, Tuttlingen, Germany) was inserted into the DCA tunnel for further supervision (specimens 1R and 1L).

Electrode Array Insertion
Four standard electrode arrays (31.5 mm, 24 platinum contacts) and 4 Flex[28] electrode arrays (28 mm, 19 platinum contacts) with free-fitting behavior were provided by the Med-El Corporation (Innsbruck, Austria). Electrode array insertion was performed manually, using CI temporal bone kit insertion instruments (Med-El Corporation) and an otological microneedle. The electrode arrays were inserted via the DCA tunnel through the RW into the scala tympani. Advancement of the electrode array was stopped as soon as an insertion resistance was detected. Total insertion duration was defined as the time between the start of the retroauricular incision for the tympanomeatal flap and completion of the array insertion. The middle ear structures were inspected during preparation and after insertion. Finally, the proximal end of the electrode array was fixed in the EAC using packing material in order to avoid dislocation during temporal bone extraction.

Imaging
For CBCT and micro-CT imaging, the temporal bones including the implanted electrode arrays as well as 3 titanium fiducial screws were excised from the heads using an oscillating saw. The specimens were trimmed to fit into a 36-mm-diameter specimen holder for micro-CT imaging. Then, high-resolution CBCT scans (ProMax 3D Max; Planmeca, Helsinki, Finland) were performed (voxel size: 150 μm isotropic; 90 kVp; 8 mA). The electrode array, the semicircular canals and the vestibule were segmented using

Fig. 2. Implanted electrode array, semicircular canals and vestibule segmented from CBCT data for insertion depth angle measurements. C = Center of electrode spiral. **a** The RW reference point is defined by the crossing of the implanted electrode array with an imaginary reference line (L_{Ref}) from the apex of the superior semicircular canal (S-SCC) through the center of the vestibule (V). **b** Same view, but superimposed onto a CBCT slice through the basal turn. The insertion depth angle (θ) is defined as the angle between L_1 and L_2, where L_1 is a line through C (perpendicular to L_{Ref}) and L_2 is the extrapolation of an imaginary line from C through the tip of the electrode array.
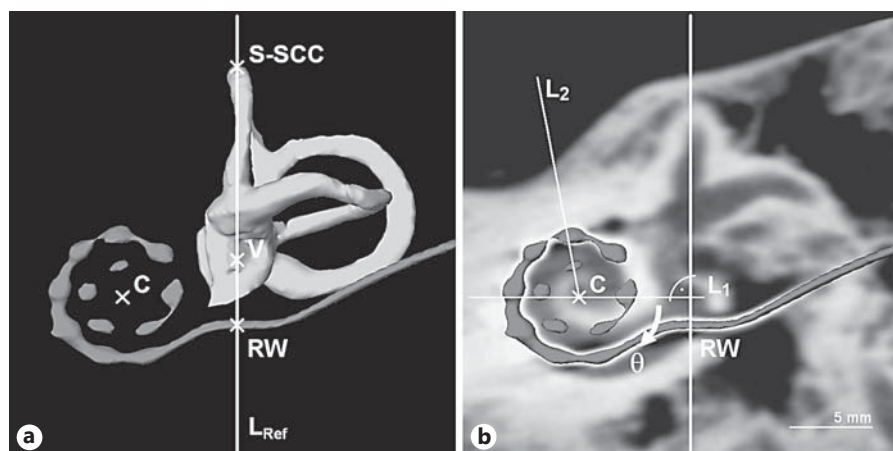
Amira 5 visualization software (VSG, Burlington, Mass., USA). The insertion depth angle (θ) of each implanted array was measured as described in Xu et al. [2000] (fig. 2). Furthermore, the DCA tunnel orientation with respect to both the basal cochlear turn (angle δ) and the direction of the electrode array in the RW (angle ε) was assessed (fig. 3). The CBCT scans were evaluated by an otolaryngologist and a neuroradiologist in order to determine the number of intracochlear contacts, the presence of array kinking and the intracochlear position of the electrode array with regard to the scala tympani, scala media or scala vestibuli in the basal, medial and apical turns of the cochlea. Complete placement of the electrode array with all contacts in the scala tympani was considered a full insertion.

The samples were additionally scanned with a micro-CT device (μCT 40; Scanco Medical AG, Brüttisellen, Switzerland) set at 70-kVp tube potential and 114-μA tube current. The dimensions of our samples limited the resolution of the scans to an isotropic voxel size of 18 μm. The electrode array was segmented and coregistered with the CBCT data using a surface alignment algorithm in Amira 5. After registration, the results found from the CBCT validation were compared and the intracochlear trauma was assessed by a neuroradiologist. For further visualization, micro-CT data were rendered as a 3D volume model.

Results

Surgery/Electrode Array Insertion

The electrodes were manually inserted through the DCA tunnel into the cochlea via the RW. Manipulation and control of the insertion process was performed using common otological surgical instrumentation through the tympanomeatal flap. Insertion was achieved without explicit difficulties in all 8 temporal bones. After the tympanomeatal flap was elevated, the RW niche was completely visible in 6 of the 8 specimens. In 2 specimens (2R/2L; table 1) about 1 mm of the EAC posterior wall was removed to adequately expose the RW niche (fig. 4). Congruency between the end of the DCA trajectory and the
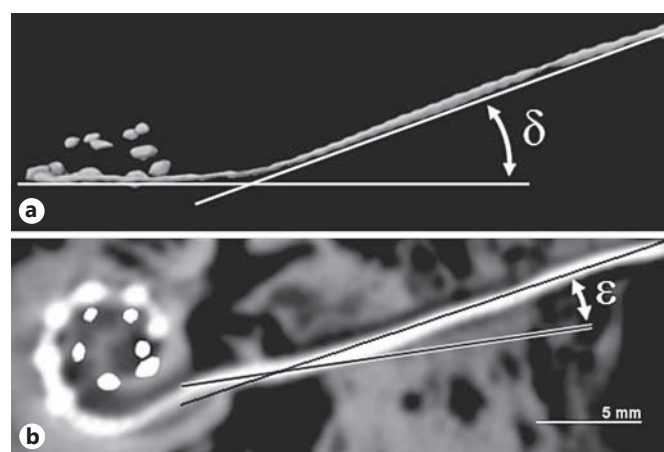

Fig. 3. DCA tunnel alignment described by the angles δ and ε, measured using CBCT scanning. **a** Axial view of the segmented electrode array implanted on the left side. Angle δ is measured between the axis of the DCA trajectory and the plane of the basal cochlear turn. **b** Coronal view of the cochlea and projected trajectory plane. The RW entry angle (ε) describes the deflection of the electrode array in the hook region of the basal turn and is measured between the axis of the DCA trajectory and the tangent of the electrode array in the center of the RW.

center of the RW as a target of the preceding study was confirmed in all cases.

After insertion, no damage to the ossicles or the chorda tympani was observed. In 5 cases, the tip of the array had to be guided to the RW opening using a microforceps/-needle. Further advancement of the electrode array after introduction into the cochlea was possible without using instrumentation in 4 specimens (table 1). Seven of the 8 insertions were full insertions, where further advancement was prevented by the silicone marker ring of the 'stan-

24   Audiol Neurotol 2014;19:22–30
DOI: 10.1159/000356165   Wimmer/Bell/Huth/Weisstanner/
Gerber/Kompis/Weber/Caversaccio

Downloaded by:
Universitätsbibliothek Bern
130.92.9.55 - 1/7/2014 4:35:25 PM

Fig. 4. Microscopic view of the tympanic cavity through the EAC during insertion in 2 different specimens. **a** The electrode array carrier (1) is manually advanced through the DCA tunnel (2) into the cochlea via the RW (3). To increase the visibility of the RW opening, approximately 1 mm of the EAC posterior wall was removed (4). The chorda tympani (5) and a fiducial screw (6) provide orientation marks. Specimen 2L. **b** The electrode array (1) is inserted into the RW and advanced when necessary using microforceps (7). The long process of the incus (8) provides an orientation landmark. Specimen 3L.
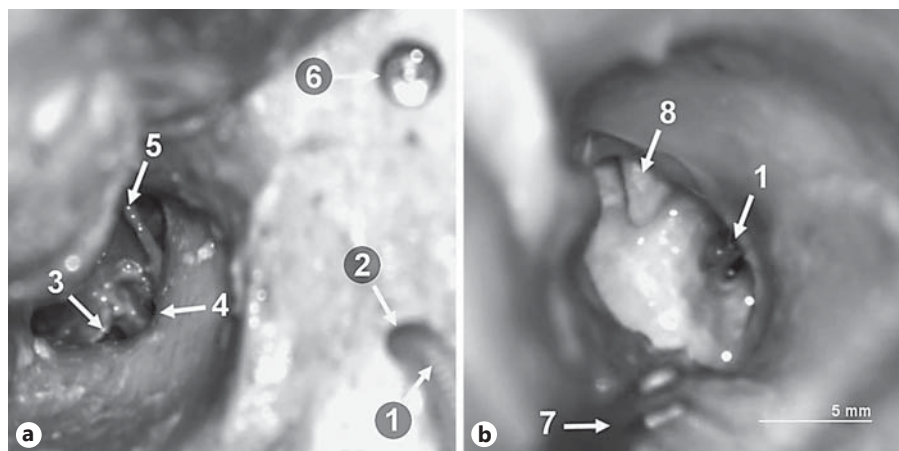
dard' array or the increased diameter of the Flex[28] array, respectively. In 1 case, 2 pairs of contacts were visible outside the cochlea when the first point of resistance was reached (specimen 3R; fig. 5c). The average total duration of the insertion procedure was found to be about 35 min, excluding the time required for DCA drilling. An improvement in absolute duration of the insertion procedure was observed over time (table 1). A movie of the manual insertion process is provided as online supplementary video 1 (for all online suppl. material, see www.karger.com/doi/10.1159/000356165).

Imaging

The cochlea of specimen 1R was damaged during preparation, making only 7 temporal bones available for further evaluation. CBCT assessment demonstrated 3 cases of complete scala tympani implantation (fig. 6a). In the medial turn of specimens 1L, 2R and 3R, the electrode array was found to be in an intermediate position at the lateral wall without clear assignability to either the scala tympani or scala media (fig. 5a). CBCT imaging showed smooth electrode array ascension and excluded any kinking. In the basal turn of specimen 4L, the basilar membrane was perforated and the array demonstrated a shift from the scala tympani into the scala vestibuli and back (table 1; fig. 7a). Three experiments conducted with the shorter Flex[28] array (27 mm length vs. 31.5 mm in the standard array) led to an overinsertion by 30–80° (specimens 2L, 4L and 4R; table 1; fig. 7c).

Evaluation of the micro-CT images confirmed the CBCT findings (table 1). Again, the electrode array of specimens 1L, 2R and 3R could not be clearly assigned to either the scala tympani or the scala media due to an intermediate position at the lateral wall in the medial turn
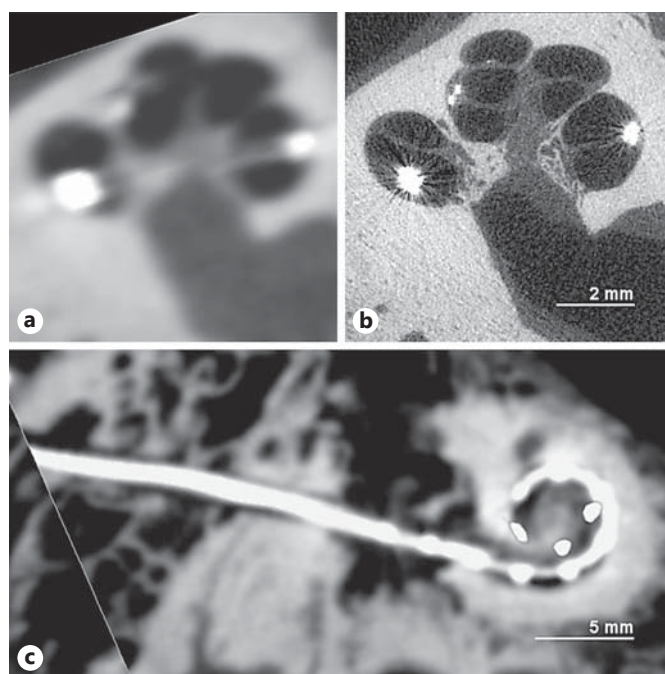

Fig. 5. Postoperative scans of the right cochlea with a partially inserted standard array in an intermediate position between the scala tympani and scala media (specimen 3R). Two pairs of electrode contacts are visible outside the cochlea. **a** Transversal CBCT image. **b** Corresponding micro-CT scan. **c** Coronal CBCT slice of the cochlear basal turn and projected DCA trajectory plane. Electrode array contacts present in the medial turn of the cochlea are overlaid.

of the cochlea (fig. 5b). The basilar membrane could be clearly identified in 6 of the 7 imaged cases; however, identification was not possible in specimen 2R. Electrode array displacement into the scala vestibuli was confirmed for specimen 4L (fig. 7b). Micro-CT data permitted 3D

Table 1. Intraoperative in vitro study results and CBCT/micro-CT validation findings

	1R	1L	2R	2L	3R	3L	4R	4L
Specimen ID								
Age, years	80	80	51	51	97	97	77	77
Gender	female	female	female	female	female	female	male	male
Intraoperative observation								
Electrode array type	standard	standard	standard	Flex[28]	standard	Flex[28]	Flex[28]	Flex[28]
Drilling of EAC wall	no drilling	no drilling	posterior (1 mm)	posterior (1 mm)	no drilling	no drilling	no drilling	no drilling
Visual check of DCA tunnel/RW alignment	microneedle and endoscope	microneedle and endoscope	microneedle	microneedle	micro-needle	micro-needle	micro-needle	micro-needle
Introduction of array tip into RW	direct/no tool	direct/no tool	microneedle	microneedle	direct/no tool	micro-forceps	micro-forceps	micro-needle
Advancement of electrode array	direct/no tool	direct/no tool	microclamp	microclamp	direct/no tool	micro-forceps	micro-forceps	direct/no tool
Total insertion duration, min	40	40	35	30	35	45	30	20
Intracochlear contacts	24 of 24	24 of 24	24 of 24	19 of 19	20 of 24	19 of 19	19 of 19	19 of 19
Postoperative CBCT validation								
Insertion depth angle θ, °	N/A	525	600	620	540	700	540	720
Scala implanted								
Basal turn	N/A	ST	ST	ST	ST	ST	ST	ST/SV
Medial turn	N/A	ST[a]	ST[a]	ST	ST[a]	ST	ST	SV/ST
Apical turn	N/A	–	–	–	–	–	–	ST
Array ascension	N/A	smooth	smooth	smooth	smooth	smooth	smooth	scala shift
DCA tunnel alignment angle δ, °	N/A	21	14	12	15	18	21	20
RW entry angle ε, °	N/A	15	10	25	5	4	18	10
Postoperative micro-CT validation								
Scala implanted								
Basal turn	N/A	ST	ST	ST	ST	ST	ST	ST/SV
Medial turn	N/A	ST/SM[a]	ST/SM[a]	ST	ST/SM[a]	ST	ST	SV/ST
Apical turn	N/A	–	–	–	–	–	–	ST
Intracochlear trauma[b]								
Basal turn	N/A	G0	G0	G0	G0	G0	G0	G3
Medial turn	N/A	G1/G2[a]	G1/G2[a]	G0	G1/G2[a]	G0	G0	G3
Apical turn	N/A	–	–	–	–	–	–	G0

1R/L to 4R/L are specimen identification numbers. ST = Scala tympani; SV = scala vestibuli; SM = scala media; – = no electrode array present; G0 = no trauma; G1 = basilar membrane displacement; G2 = basilar membrane rupture; G3 = dislocation into SV; N/A = not available.
[a] Not determinable; intermediate position between ST and SM. [b] Grading scale [Eshraghi et al., 2003].

rendering of the implanted specimens (fig. 8). However, the 3D rendering to this point has provided no further insight into visualization of the basilar membrane (specimen 2R) or determination of the exact location of the intermediately positioned electrode arrays.

Discussion

This study investigated the feasibility and efficacy of inserting a free-fitting CI electrode array through a minimally invasive DCA tunnel. The hypothesis that a complete array insertion through the DCA tunnel can be suc-

cessfully performed by utilizing common otological instrumentation was confirmed. The implanted electrode array position and DCA tunnel alignment were evaluated on postoperative CBCT images, and corresponding micro-CT data permitted an assessment of intracochlear insertion trauma.

To our knowledge this is the first report of a CI insertion study conducted on Thiel embalmed specimens. This conservation technique is considered to realistically reproduce the color, mobility and flexibility of tissues in intraoperative situations and to offer excellent conditions for the training of surgical procedures in otology [Alberty et al., 2002]. Negative aspects of the Thiel fixa-
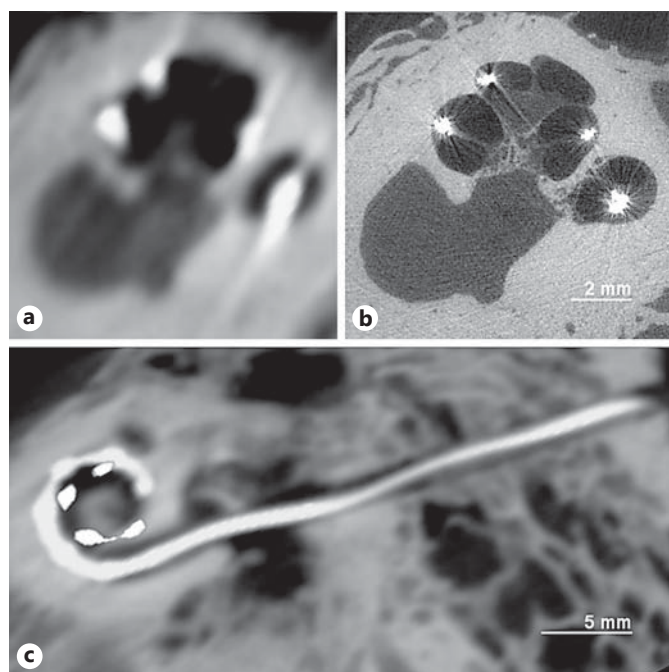
Wimmer/Bell/Huth/Weisstanner/
Gerber/Kompis/Weber/Caversaccio

Fig. 6. Postoperative scans of the left cochlea, demonstrating atraumatic scala tympani insertion of a Flex[28] array (specimen 3L). **a** Transversal CBCT image. **b** Corresponding micro-CT scan. **c** Coronal CBCT slice of the cochlear basal turn and projected DCA trajectory plane. Electrode array contacts present in the medial turn of the cochlea are overlaid.
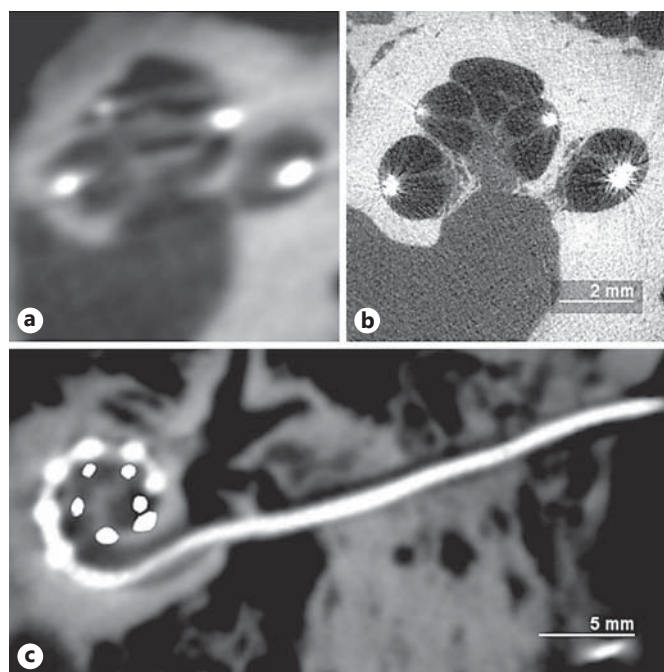
Fig. 7. Postoperative scans of the left cochlea with overinserted Flex[28] array and basilar membrane rupture caused by dislocation of the array into the scala vestibuli in the medial cochlear turn (specimen 4L). **a** Transversal CBCT image. **b** Corresponding micro-CT scan. **c** Coronal CBCT slice of the cochlear basal turn and projected DCA trajectory plane. Electrode array contacts present in the medial turn of the cochlea are overlaid.

Fig. 8. 3D micro-CT data rendering of specimen 2L. **a** Magnified view of the tympanic cavity and the proximal portion of the EAC, showing the malleus (MA), incus (IN) and stapes (ST), as well as the electrode array (EA) entering through the RW. **b** Coronal view of the same specimen, demonstrating the course of the implanted EA through the DCA tunnel and the RW into the cochlea. An animated version of the 3D model is provided as online supplementary video 2.
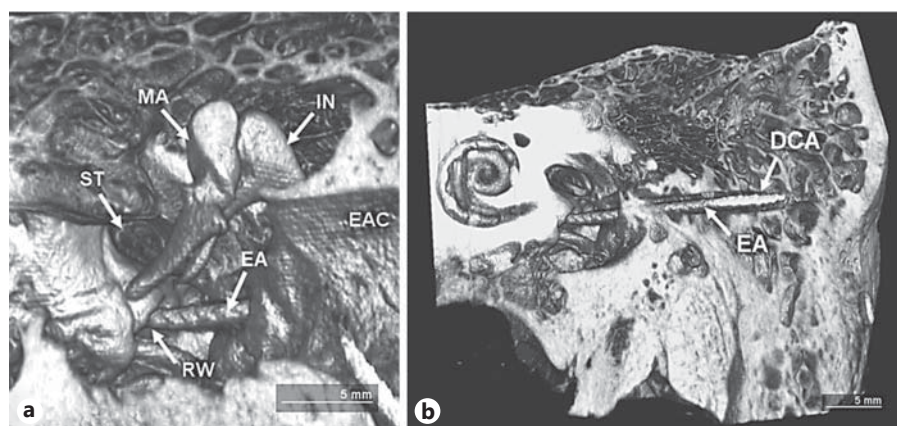
tion are bad conservation of organs like the brain or bone marrow and the gelatinous texture of certain soft tissues (e.g. cartilage) [Benkhadra et al., 2011]. Generally, micro-CT assessment showed good preservation of intracochlear structures. In 1 case, the basilar membrane was not visible (specimen 2R). However, because the course of the electrode array implies the presence of a basilar membrane, we assume that this was caused by imaging artifacts. Further, we experienced little resistance during insertion, which may be related to the fixation method and explain the deep insertions achieved in this study. Therefore, we suggest further histological analysis to verify the applicability of the Thiel fixation method.

A tympanomeatal flap (routine for tympanic cavity access) as performed in this study is an additional step not common to the normal facial recess approach. Thus, the application of a tympanomeatal flap increases the risk of tympanic membrane perforation, subsequent electrode array exposure and middle/inner ear infections as compared with the standard approach. In this work, the tympanomeatal flap approach provided sufficient visual exposure to perform microscopic procedures such as cochleostomy drilling and sealing. The creation of the tympanomeatal flap accounts for an additional time of 15 min when compared with conventional insertion. Additionally, the tympanomeatal flap could be elevated prior to and for supervision of the tunnel drilling. Microscopic inspection and probing with an otological microneedle allows for sufficient evaluation of DCA tunnel target alignment with the RW niche. An alternative method might be direct endoscopic inspection and evaluation of DCA tunnel target alignment. Due to the suboptimal resolution of the sialendoscope, microscopic inspection was preferred in this study.

Previous studies have reported on the clinical applicability of CBCT petrous bone imaging for postoperative assessment of CI array positions. CBCT imaging is favorable due to its submillimeter spatial resolution and fast acquisition time (<20 s). Furthermore, CBCT has reduced radiation exposure compared with conventional multislice CT imaging [Cushing et al., 2012; Kurzweg et al., 2010]. The imaging resolution is, however, insufficient for the assessment of intracochlear trauma, and the radiologically measured electrode array diameter is exaggerated due to imaging artifacts [Güldner et al., 2012]. We observed that the CBCT scans provided a sufficient image resolution and quality for estimation of the implanted scala in all cases imaged (table 1). However, in 3 cases the electrode array was observed to be in the region of the scala media (specimens 1L, 2R and 3R, all standard arrays; fig. 5a). This intermediate position of the array, also described in Teymouri et al. [2011], may refer to either a basilar membrane elevation with the array still being present in the scala tympani or even a perforation with a shift into the scala media. CBCT evaluation demonstrated that the DCA tunnel was not fully aligned with the basal turn of the cochlea in any specimen (angle δ; table 1). While an optimized alignment may contribute to a reduction in insertion trauma, the results of this study do not suggest a correlation between trauma and the out-of-plane (δ) or in-plane (ε) components of the insertion angle. In many cases, the positions of structures of the facial recess, and an RW approach, will certainly limit an optimized insertion angle (minimization of δ and ε). Likewise, more optimal insertion angles could be achieved in some cases by abandoning the RW insertion in favor of a cochleostomy, which may lead to a reduction in insertion force, as proposed by Meshik et al. [2010]. A strict RW insertion approach combined with the use of free-fitting electrode arrays resulted in bending at the RW entrance and the hook region of the basal turn of the cochlea, mainly in specimens 2R, 2L, 4R and 4L (fig. 7c). Interestingly, this bending did not seem to cause additional trauma, and the electrode insertion was perceived as smooth.

In this study, micro-CT scans were obtained to overcome the aforementioned limitations of CBCT imaging and to assess intracochlear trauma. Micro-CT may provide sufficient spatial resolution to display intracochlear membranous structures, but it is limited to in vitro examinations of small samples. Overall, the findings of the micro-CT evaluation matched the outcome of the CBCT investigation. Assessment of the micro-CT data confirmed 3 cases to be atraumatic scala tympani insertions (specimens 2L, 3L and 4R, all Flex[28] arrays; fig. 6b). The image quality was not sufficient to resolve the difference between displacement and perforation and to estimate the exact intracochlear position of the electrode arrays in the intermediate position. Therefore, the intracochlear insertion trauma should be interpreted with caution and definitive evidence of atraumatic insertion cannot be obtained without further histological analysis of specimens 1L, 2R and 3R. The extent of intracochlear trauma was similar when compared with the results of previous temporal bone insertion studies with free-fitting electrode arrays (array length: ≥25 mm) [Adunka et al., 2004; Adunka and Kiefer, 2006; Skarzynski and Podskarbi-Fayette, 2010]. These studies report 25–27% of cases exhibiting basilar membrane/spiral ligament displacement or perforation, 0–9% of cases with dislocation of the array into the scala vestibuli, and 5–33% of cases with modiolus/osseous spiral lamina fracture, compared with 43, 14 and 0%, respectively, in this study. In this work, deep insertions were achieved with nearly all arrays inserted more than one and a half turns (θ ≥ 540°; table 1). The mean insertion depth angle of 606° by far exceeds the values estimated in the studies reviewed (325–461°). Nevertheless, a similar percentage of atraumatic insertion cases (43% compared with 33–59% reported in the literature) was found. Considering a hypothetical functionality of intracochlear contacts in specimens 2R and 3R, the electrodes near the RW would most probably provide no contribution to cochlear stimulation (fig. 5c).

In conclusion, manual electrode array insertion following a minimally invasive mastoidectomy with supervision through a tympanomeatal flap is feasible and effective. In regard to electrode array insertion and imaging quality, Thiel-fixed temporal bones appear to be an adequate model for cochlear electrode insertion studies. The insertion depths achieved by this method were greater than those in the literature and should be considered when aiming for residual hearing preservation. Regarding trauma assessment, the approach presented cannot be truly compared with the current gold standard (conventional facial recess approach), although this may be achievable with further research into patient-specific insertion angle optimization. However, exclusively free-fitting electrode arrays were investigated in this study in an RW approach, and similar insertion investigations will be required in order to evaluate the nuances of cochleostomy access and perimodiolar arrays with associated insertion tools.

The implantation technique presented must be considered within the context of the associated clinical workflow required for minimally invasive robotic CI surgery. Based on the results of a previous in vitro study [Bell et al., 2013] and currently undergoing investigations within the clinical environment, a total procedural time of about 2 h is estimated for minimally invasive robotic cochlear implantation. Preoperative steps are fiducial screw implantation under local anesthesia (20 min), preoperative CBCT imaging (10 min) and subsequent trajectory planning (15 min). An intraoperative time of about 75 min is aimed for in the final state of the workflow, consisting of robotic system setup (15 min), patient preparation and registration (20 min), DCA drilling (5 min) and the implantation procedure presented in this study (35 min). The implant receiver can be fixed using any favored conventional technique including milling an implant bed and/or tie-down of the implant body. The electrode array can be inspected intraoperatively via the tympanomeatal flap, such as in case of acute implant failure. Likewise, management of cerebrospinal fluid gushers can be achieved through the tympanomeatal flap, for example by using soft tissue packing (gelfoam, fat) and fibrin glue. It has yet to be seen to what extent postoperative scar formation occurs, but revisions may need to be performed under a conventional mastoidectomy and posterior tympanotomy.

In light of a future commercialization, the question of costs and benefits associated with the DCA procedure arises. Potential benefits like reduced invasiveness, shorter intraoperative time and possibility of outpatient treatment must be weighed against the substantial costs of such a system, which would greatly vary in different countries and cannot be specified within the scope of this work.

References

Adunka O, Kiefer J: Impact of electrode insertion depth on intracochlear trauma. Otolaryngol Head Neck Surg 2006;135:374–382.

Adunka O, Unkelbach MH, Mack M, Hambek M, Gstoettner W, Kiefer J: Cochlear implantation via the round window membrane minimizes trauma to cochlear structures: a histologically controlled insertion study. Acta Otolaryngol 2004;124:807–812.

Alberty J, Filler TJ, Schmäl F, Peuker ET: Thiel method fixed cadaver ears: a new procedure for graduate and continuing education in middle ear surgery (in German). HNO 2002; 50:739–742.

Balachandran R, Mitchell JE, Blachon G, Noble JH, Dawant BM, Fitzpatrick JM, Labadie RF: Percutaneous cochlear implant drilling via customized frames: an in vitro study. Otolaryngol Head Neck Surg 2010;142:421–426.

Baron S, Eilers H, Munske B, Toennies JL, Balachandran R, Labadie RF, Ortmaier T, Webster RJ 3rd: Percutaneous inner-ear access via an image-guided industrial robot system. Proc Inst Mech Eng H 2010;224:633–649.

Bell B, Gerber N, Williamson T, Gavaghan KA, Wimmer W, Caversaccio M, Weber S: In vitro accuracy evaluation of image-guided robot system for direct cochlear access. Otol Neurotol 2013;34:1284–1290.

Benkhadra M, Gérard J, Genelot D, Trouilloud P, Girard C, Anderhuber F, Feigl G: Is Thiel's embalming method widely known? A world survey about its use. Surg Radiol Anat 2011; 33:359–363.

Cushing SL, Daly MJ, Treaba CG, Chan H, Irish JC, Blaser S, Gordon KA, Papsin BC: High-resolution cone-beam computed tomography: a potential tool to improve atraumatic electrode design and position. Acta Otolaryngol 2012;132:361–368.

Eshraghi AA, Yang NW, Balkany TJ: Comparative study of cochlear damage with three perimodiolar electrode designs. Laryngoscope 2003;113:415–419.

Gerber N, Bell B, Gavaghan K, Weisstanner C, Caversaccio M, Weber S: Surgical planning tool for robotically assisted hearing aid implantation. Int J Comput Assist Radiol Surg 2013a, E-pub ahead of print.

Gerber N, Gavaghan K, Bell B, Williamson T, Weisstanner C, Caversaccio M, Weber S: High accuracy patient-to-image registration for the facilitation of image-guided robotic microsurgery on the head. IEEE Trans Biomed Eng 2013b;60:960–968.

Güldner C, Wiegand S, Weiss R, Bien S, Sesterhenn A, Teymoortash A, Diogo I: Artifacts of the electrode in cochlea implantation and limits in analysis of deep insertion in cone beam tomography (CBT). Eur Arch Otorhinolaryngol 2012;269:767–772.

Hiraumi H, Yamamoto N, Sakamoto T, Ito J: A minimally invasive approach for cochlear implantation using a microendoscope. Eur Arch Otorhinolaryngol 2013;270:477–481.

Hussong A, Rau TS, Ortmaier T, Heimann B, Lenarz T, Majdani O: An automated insertion tool for cochlear implants: another step towards atraumatic cochlear implant surgery. Int J Comput Assist Radiol Surg 2010;5:163–171.

Klenzner T, Ngan CC, Knapp FB, Knoop H, Kromeier J, Aschendorff A, et al: New strategies for high precision surgery of the temporal bone using a robotic approach for cochlear implantation. Eur Arch Otorhinolaryngol 2009;266:955–960.

Kobler JP, Kotlarski J, Oltjen J, Baron S, Ortmaier T: Design and analysis of a head-mounted parallel kinematic device for skull surgery. Int J Comput Assist Radiol Surg 2012;7:137–149.

Kratchman LB, Blachon GS, Withrow TJ, Balachandran R, Labadie RF, Webster RJ 3rd: Design of a bone-attached parallel robot for percutaneous cochlear implantation. IEEE Trans Biomed Eng 2011;58:2904–2910.

Kratchman LB, Schurzig D, McRackan TR, Balachandran R, Noble JH, Webster RJ 3rd, Labadie RF: A manually operated, advance off-stylet insertion tool for minimally invasive cochlear implantation surgery. IEEE Trans Biomed Eng 2012;59:2792–2800.

Kurzweg T, Dalchow CV, Bremke M, Majdani O, Kureck I, Knecht R, Werner JA, Teymoortash A: The value of digital volume tomography in assessing the position of cochlear implant arrays in temporal bone specimens. Ear Hear 2010;31:413–419.

Labadie RF, Noble JH, Dawant BM, Balachandran R, Majdani O, Fitzpatrick JM: Clinical validation of percutaneous cochlear implant surgery: initial report. Laryngoscope 2008;118:1031–1039.

Meshik X, Holden TA, Chole RA, Hullar TE: Optimal cochlear implant insertion vectors. Otol Neurotol 2010;31:58–63.

Skarzynski H, Podskarbi-Fayette R: A new cochlear implant electrode design for preservation of residual hearing: a temporal bone study. Acta Otolaryngol 2010;130:435–442.

Teymouri J, Hullar TE, Holden TA, Chole RA: Verification of computed tomographic estimates of cochlear implant array position: a micro-CT and histological analysis. Otol Neurotol 2011;32:980–986.

Thiel W: The preservation of the whole corpse with natural color (in German). Ann Anat 1992;174:185–195.

Xu J, Xu S, Cohen L, Clark G: Cochlear view: postoperative radiography for cochlear implantation. Am J Otol 2000;21:49–56.

Zeitler DM, Balkany TJ: Alternative approaches to cochlear implantation. Oper Tech Otolaryngol 2010;21:248–253.